IEEE Access
Multidisciplinary : Rapid Review : Open Access Journal

Received 8 February 2024, accepted 8 March 2024, date of publication 18 March 2024, date of current version 25 March 2024.

Digital Object Identifier 10.1109/ACCESS.2024.3377250

RESEARCH ARTICLE

Multi-Objective Optimal Energy Management of Nanogrid Using Improved Pelican Optimization Algorithm

SAIF JAMAL [1], JAGADEESH PASUPULETI [2], (Senior Member, IEEE), NUR AZZAMMUDIN RAHMAT [3], AND NADIA M. L. TAN [4,5], (Senior Member, IEEE)

[1]Department of Electrical and Electronics Engineering, College of Engineering, Universiti Tenaga Nasional, Kajang, Selangor 43000, Malaysia
[2]Institute of Sustainable Energy, Universiti Tenaga Nasional, Kajang, Selangor 43000, Malaysia
[3]Department of Electrical Power Engineering, Universiti Tenaga Nasional, Kajang, Selangor 43000, Malaysia
[4]Key Laboratory of More Electric Aircraft Technology of Zhejiang Province, University of Nottingham, Ningbo 315100, China
[5]Institute of Power Engineering, Universiti Tenaga Nasional, Kajang 43000, Malaysia

Corresponding authors: Saif Jamal (saif.milan227@gmail.com) and Jagadeesh Pasupuleti (Jagadeesh@uniten.edu.my)

This work was supported by the Ministry of Higher Education, Malaysia, through the Fundamental Research Grant Scheme (FRGS) under Grant FRGS/1/2022/TK08/UNITEN/01/3 and Grant 20221002FRGS.

ABSTRACT The development of efficient energy management for nanogrid (NG) systems, while reducing both the carbon dioxide (CO_2) emissions and power generation cost, is achievable through the effective utilization of available energy sources. This paper proposes a multi-objective optimal energy management strategy for grid-connected NG systems, which incorporates PV arrays and battery storage devices (BSDs), to reduce operating costs and CO_2 emission simultaneously over a 24-hour scheduling period. This strategy, which is based on the improved pelican optimization algorithm (IPOA), involves the development of a multi-objective optimization (MOA) equation with several constraints, while taking into account the Malaysian grid purchasing and selling prices. An innovative IPOA-derived technique is developed to facilitate the NG's optimal energy management operation in multi-objective situations. The proposed algorithm is tested on three distinct scenarios to affirm its efficacy. It is assumed that (a) power exchange between the NG and the main grid is limitless, (b) power interchange between the NG and main grid has a predetermined limit and (c) operating at the maximum capacity of PV array. In order to demonstrate the effectiveness of the proposed algorithm, The outcomes of the simulation are juxtaposed with results obtained from the initial Pelican Optimisation Algorithm (POA), the Bat Algorithm, and the Improved Differential Evolutionary (IDE) Algorithm. The simulation reveals that the suggested IPOA algorithm exhibited the most economical performance and the lowest CO_2 emissions. Moreover, in the second scenario, operational costs decreased by 9.5%, and CO_2 emissions were reduced by 15%. Conversely, in Scenario 3, there was a 2% decrease in cost and 23% reduction in CO_2 emissions as against the first scenario.

INDEX TERMS Nanogrid, multi-objective energy management, IPOA, optimization, cost effective, CO_2 emission.

I. INTRODUCTION

Of late, the use of nanogrids (NGs) and microgrids (MGs) for delivering superior power quality through the utilization of wind and solar energy sources while simultaneously reducing greenhouse gas emissions and increasing service reliability has drawn the attention of players in the electrical power industry [1]. The emission of pollutants into the atmosphere, stemming from the rapidly growing demand for electrical power, is currently viewed as a global concern [2]. The emergence of NGs and MGs as important power distribution systems is attributed to their capacity for combining

The associate editor coordinating the review of this manuscript and approving it for publication was Qiang Li.

multiple distribution sources, including energy storage devices (ESDs), and renewable as well as non-renewable energy sources [3]. The power pyramid portrays the primary distinctions between NGs and MGs. For instance, according to the power pyramid, in comparison to MGs, NGs come with a lower power level and are less intricate. With a power output of tens of MW, MGs are capable of providing electricity to heavy consumption locations such as universities, hospitals, and industrial units. Nanogrids (NGs), on the other hand, with a magnitude of tens of KW, are utilized for single-family homes or small structures [4], [5].

Many aspects of the MG and NG systems, with the emphasis on energy scheduling and optimal management, are documented in literature relevant to this subject matter. Several studies delved into single-objective optimizations, focusing on the reduction of MG and NG operating costs, through the appropriate management of generation units to achieve the best possible economic outcome. For example, in [6], the authors introduce the recursive particle swarm optimization (RPSO) algorithm which strives to reduce the overall cost of the NG by optimizing the use of RES and decreasing the use of traditional sources such as microturbines (MTs) and diesel generators (DGs). According to the test results, in comparison to the bat and genetic algorithms (GAs), the proposed algorithm is more effective. On the downside, however, in terms of addressing the problem, the proposed technique required a longer period than the bat and GA algorithms. The authors in [7] present the herd optimization algorithm (HOA) for stand-alone NG short-term scheduling with the objective of reducing operation costs, while taking fuel limits into consideration. According to the simulation results, in comparison to other alternative methods, their recommended algorithm delivers a superior outcome. In [8] and [9], the authors put forward an economic dispatch (ED) problem for grid-connected microgrids to maximize the use of RES and minimize the dependence on non-renewable energy sources in order to arrive at the best possible economic circumstance.

Several scholars examined multi-objective optimization (MOA) problems involving both economic and environmental energy management in MGs. In [10], a fuzzy self-adaptive particle swarm optimization (FSAPSO) technique is introduced to manage the multi-objective problem of economy and emission for a grid-connected MG made up of a wind turbine (WT), a photovoltaic array, a microturbine, a fuel cell (FC), and a battery storage device (BSD). In order to minimize both the MG's emissions and overall operating costs, a nonlinear optimization problem was developed for the multi-objective problem. The limitations were taken into consideration during this exercise. A comparison with the FSAPSO, PSO, and GA revealed that, in terms of cost and emission minimization, the recommended algorithm performs better.

In [11], a multi-objective PSO algorithm is employed to achieve the best allocation and management of energy resources in a grid-connected MG made up of a WT, a PV array, a MT, a FC, and a BSD. The goal is to concurrently minimize the MG's emission and overall operation costs through nonlinear optimization. In order demonstrate the effectiveness of the multi-objective PSO algorithm it was compared with the non-dominated sorting genetic algorithm (NSGA-II). The authors in [12] introduce a modified tribe-PSO approach for addressing multi-objective challenges in grid-connected microgrids with the objective of simultaneously reducing emissions and operational costs. The effectiveness of this adapted algorithm is verified through a comparison with the original PSO.

In [13], a dual-objective approach based on NSGA-II is employed to reduce both carbon dioxide (CO_2) emissions and the net percentage cost. This approach takes into account the energy expenses, annualized capital costs, and life cycle costs as well as the operation and maintenance costs (O&M) for grid-connected microgrids. The inclusion or exclusion of BSDs was explored with the most favorable results in terms of cost and CO_2 emission minimization deriving from the use of BSDs together with RES.

A refined iteration of the sparrow search algorithm (SSA) was introduced as an approach for managing grid-connected microgrids comprising a WT, PV array, FC, MT, and BSDs. Two distinct optimization challenges were addressed. The first challenge has to do with the specific objective of reducing either the overall CO_2 emissions, or the total operational costs of the microgrid, while the second challenge, which is multi-objective in nature, concerns the minimization of both the overall emissions and the aggregate operating costs of the MG. According to the test results, in addressing the single objective challenge, the proposed algorithm successfully achieved a 54.76% reduction in emissions and a 1.44% decrease in costs as against the krill herd optimizer (KHO). Conversely, in the context of the multi-objective challenge, the SSA algorithm excels by reducing emissions by 0.118% and achieving savings of approximately 42.78% in operating costs when compared to the ant lion optimizer (ALO) [14].

In the context of NG applications, the use of a MOA aimed at reducing both cost and CO_2 emission is hampered by the issue of different distributed sources. The economical and efficient operation of the NG system poses a significant challenge due to the need for effective management and scheduling of various sources. Despite several approaches and strategies proposed for MG management, the utilization of metaheuristic optimization approaches in this field is limited. This constraint emphasises the need for increased attention and application in this domain. The importance of this is further emphasised by the proven effectiveness of metaheuristic optimization approaches in various areas related to renewable energy [15], [16]. Therefore, there is a need for a more extensive assimilation and exploration of these methodologies from the perspective of MG and NG operations to fully leverage their likely benefits.

This study focuses on the application of an enhanced algorithm, known as the pelican optimization algorithm

(POA), an algorithm inspired by the hunting behavior of pelicans, to optimize energy management and scheduling for grid-connected NG systems with the dual objective of minimizing both operating costs and the emission of CO_2. With this paper, we comprehensively outline the steps involved with regards to the POA and the improved version designated the IPOA, providing mathematical models for both. In terms of power exchange between the NG system and the main grid, we considered three distinct scenarios: first one with unrestricted power exchange and second one with limited power exchange and third Scenario with maximum operating capacity of PV source. Market pricing (buying/selling) is taken into consideration for this power exchange. To showcase the effectiveness of the recommended algorithm, the performance of IPOA is compared to that of the original POA, the improved differential evolutionary (IDE) algorithm [17], and the bat algorithm [18]. This paper's key contributions can be succinctly outlined as follows:

1) Introduction of the Pelican Optimization Algorithm, a novel approach for optimal control and management of NG energy.
2) The algorithm proposed demonstrates notable attributes, including rapid convergence, straightforward construction, and minimal control parameters.
3) Analysis of multi-objective optimization problems focusing on minimizing both total operating cost and CO_2 emissions.
4) Introduction of an improvement to the Pelican Optimization Algorithm tailored for solving multi-objective optimization problems.
5) Conducting a comparative assessment with the IDE and Bat Algorithm.
6) Affirmation of the robustness and efficacy of the proposed IPOA in the context of multi-objective optimization.

The paper is structured as follows: Section I presents the introduction and literature review regarding NG and MG energy management, Section II delves into the problem formulation, including the two objective functions, limitations, and NG modelling, Section III presents an explanation on the proposed optimization algorithm, while Section IV discloses the simulation results. The conclusions are provided in Section V.

II. PROBLEM FORMULATION

In this section, we focus on the optimization of energy management and scheduling with regards to NG by way of a MOA approach, while taking the economic and environmental aspects into consideration. NG modelling and the proposed POA are also discussed in this section. In the multi-objective framework, both goals, namely the reduction of the overall CO_2 emission and the minimization of operating costs are addressed concurrently, while complying with the limitations of the NG system. Subsequently, the problems are formulated as follows.

A. OBJECTIVE FUNCTIONS

The task of optimizing power distribution for economic and environmental purposes as well as the management of NG system operations can be framed as a MOA model.

In this process, it is essential that the dual objective of reducing the NG system's overall CO_2 emission and the minimizing of the overall operating costs be achieved simultaneously, while adhering to the system constraints. The mathematical representation of this problem is as follows.

1) MINIMIZING THE TOTAL COSTS OF OPERATING IN NG

The following function was proposed to decrease the total operational cost of the NG:

$$MinF_1(x) = Min \sum_{h=1}^{T} [C_{PV}(h) + C_{Bat}(h) + C_{Grid}(h)] \quad (1)$$

where, T is the duration of the entire experiment in hours (h); $C_{PV}(h)$, $C_{Bat}(h)$, and $C_{Grid}(h)$ are the cost of PV, battery and grid at hour h respectively. The operating costs of PV, battery and grid can be calculated as the following equations:

$$C_{PV}(h) = U_{PV}(h) \times P_{PV}(\text{ h}) \times B_{PV}(h) \quad (2)$$

$$C_{Bat}(h) = \sum_{j=1}^{N_B} \left(U_{Batj}(h) \times P_{Batj}(h) \times B_{Batj}(h)\right) \quad (3)$$

$$\begin{aligned} C_{Grid}(h) = \big[&P_{G,Buy}(h) \times B_{G,B\ uy}(h) \\ &-P_{G,Sell}(h) \times B_{G,Sell}(h)\big] \end{aligned} \quad (4)$$

where, N_B is the number of BSDs; $U_{PV}(h)$ and $U_{Batj}(h)$ are the status of the PV generator and BSDs at time h respectively, either in the ON or OFF modes; $P_{PV}(h)$ and $P_{Batj}(h)$ are the PV generator and BSDs' power output at time h respectively; $B_{PV}(h)$ and $B_{Batj}(h)$ are the price of PV- generated and BSD- generated energy at time h respectively; $P_{G,B\ uy}(h)$ and $P_{G,Sell}(h)$ are the amount of energy bought from, or sold to, the main energy grid at time h respectively; while $B_{G,B\ uy}(h)$ and $B_{G,S\ ell}(h)$ are the price of buying from, or selling energy to, the main energy grid at time h respectively. X is the vector of the variables, such as the energy produced by the units and their related states, which can be defined by way of the following equations:

$$\begin{aligned} X &= \left[P_g, U_g\right]_{1\times 2\ nT} \\ P_g &= [P_{PV}, P_{Bat}] \\ n &= 1 + N_B + 1 \end{aligned} \quad (5)$$

In Equation (5), T is the duration of the entire experiment, n is the number of varying states, P_g is the amount of energy produced by all the units, U_g is the vector defining the ON/OFF states of all the units at every hour of the day. All of these variables are listed in Equation (6).

$$P_{PV} = [P_{PV}(1), P_{PV}(2), P_{PV}(h), \ldots\ldots\ldots P_{PV}(T)]$$
$$P_{Bat} = \left[P_{Bat1}, P_{Bat2}, P_{Bat3}, \ldots\ldots\ldots P_{Bat,N_B}\right]$$

$$P_{Batj} = \left[P_{Batj}(1), P_{Batj}(2), P_{Batj}(h), \ldots\ldots\ldots P_{Batj}(T)\right]; \quad j = 1, 2, \ldots . N_B \tag{6}$$

where, $P_{PV}(h)$ and $P_{Batj}(h)$ are the amount of energy delivered by the PV generator and the BSD at time h respectively.

2) MINIMIZING THE TOTAL AMOUNT OF CO_2 EMISSIONS IN NG

The following function was proposed to decrease the total CO_2 emitted by the NG system:

$$Min\ F_2(x) = Min \sum_{h=1}^{T} \left[CO_2E_{Bat}(h) + CO_2E_{Grid}(h)\right] \tag{7}$$

where, $CO_2\ E_{Bat}(h)$, and $CO_2\ E_{Grid}(h)$ are the CO_2 emission of battery and grid at hour h respectively. The CO_2 emissions of battery and grid can be calculated as the following equations:

$$CO_2E_{Bat}(h) = \sum_{j=1}^{N_B} \left[U_{Batj}(h) \times P_{Batj}(h) \times EF_{Batj}(h)\right] \tag{8}$$

$$CO_2E_{Grid}(h) = P_{G,Buy}(h) \times EF_G(h) \tag{9}$$

where, $EF_{Batj}(h)$ and $EF_G(h)$ are the emission factors attributable to the BSDs and the grid at time h in kg/kWh, respectively.

B. CONSTRAINTS

1) LOAD BALANCE

The main concern is the capacity to meet the energy demand through the effective exploitation of available power sources. The power equilibrium condition within the NG system is expressed as follows:

$$\sum_{j=1}^{N_B} P_{Batj}(h) + P_{PV}(h) + P_{Grid}(h) = P_{Load}(h) \tag{10}$$

where, $P_{\text{Load}}(h)$ is the load required at time h.

2) POWER LIMITATIONS OF UNITS

All the components; namely the PV, main grid, and BSDs; come with predefined lower and upper power generation thresholds.

$$\begin{aligned} P_{PV,MIN}(h) &\le P_{PV}(h) \le P_{PV,MAX}(h) \\ P_{Batj,MIN}(h) &\le P_{Batj}(h) \le P_{Batj,MAX}(h) \\ P_{Grid,MIN}(h) &\le P_{Grid}(h) \le P_{Grid,MAX}(h) \end{aligned} \tag{11}$$

where, $P_{PV,MIN}(h)$, $P_{Batj,MIN}(h)$, and $P_{Grid,MIN}(h)$ are the minimal amount of energy produced by the PV, BSDs, and the grid, respectively, while $P_{PV,MAX}(h)$, $P_{Batj,MAX}(h)$, and $P_{Grid,MAX}(h)$ are the maximal energy produced by the PV, BSDs, and the grid, respectively.

3) CHARGING AND DISCHARGING LIMITS OF BATTERY STORAGE UNIT

$$\begin{aligned} SOC_{Bat,j}(h) &= SOC_{Bat,j}(h-1) + P_{CH/DCH}(h) \\ 0 &\le \left|P_{CH/DCH}(h)\right| \le P_{CDBatj,MAX} \end{aligned} \tag{12}$$

where, $SOC_{Bat,j}(h)$ and $SOC_{Bat,j}(h-1)$ are the volume of charging presently and previously required by the BSD, respectively, $P_{CH/DCH}(h)$ is the amount of energy charged/discharged at time h, and $P_{CDBatj.MAX}$ is the BSD's maximal rate of energy charging/discharging.

C. NANOGRID MODELING

A NG system is a combination of renewable and non-renewable energy generation sources supported with an energy storage setup [19]. These elements interconnect and engage in energy exchange with the primary grid. All these resources have the capacity to strategize and make decisions on energy generation-related issues. The performance of these control mechanisms is facilitated by a combination of local and central controllers operating within the NG framework [20]. Figure 1 portrays the NG system considered for this study, featuring the engagement of a PV array together with a BSD comprising three batteries. The NG also comes with the capacity to engage in power exchange with the main grid.

III. PRINCIPLES OF PELICAN OPTIMIZATION ALGORITHM AND MULTI-OBJECTIVE OPTIMIZATION

Real-world optimization scenarios include the presence of multiple objective functions, which require simultaneous optimization. However, this process is hampered by the fact that the objectives are not directly proportionate but, instead, are in conflict with each other [21]. The application of MOA techniques proved to be effective for attaining a set of optimal solutions to address this issue of conflicting objectives. In this segment, we provide an explanation on the core principles of our proposed IPOA, designed for optimizing energy management in NG systems. The problem at hand is expressed as:

$$\begin{aligned} &Min\ F = [f_1(X), f_2(X), \ldots, f_N(X)]^T \\ &\text{Subject to}: \\ &\begin{cases} g_i(X) < 0 & i = 1, 2, \ldots, N_{ueq} \\ h_i(X) = 0 & i = 1, 2, \ldots, N_{eq} \end{cases} \end{aligned} \tag{13}$$

where, F is the vector of the objective function, X is the vector of the optimization variable, $f_i(X)$ is the ith objective function, $g_i(X)$ is the equality limitation, $h_i(X)$ is the inequality limitation, and N is the number of objective functions.

The attainment of the optimal Pareto solutions is followed by the selection of the solution which is most appropriate. To accomplish this goal, we employed a fuzzy decision-making function incorporating a membership function which precisely determines variable values [12]. This

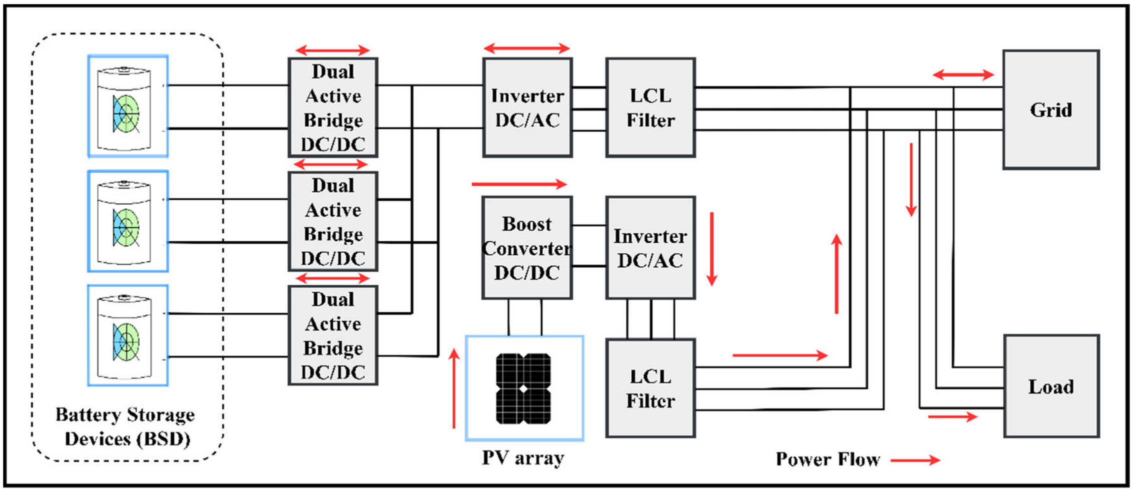

FIGURE 1. The modelling of the NG.

process is expressed in Equation (14):

$$\mu_i^k = \begin{cases} 1, & f_i \le f_i^{min} \\ \dfrac{f_i^{max} - f_i}{f_i^{max} - f_i^{min}}, & f_i^{max} < f_i < f_i^{min} \\ 0, & f_i \ge f_i^{max} \end{cases} \tag{14}$$

where, μ_i^k is the optimal objective function of i in the k-optimal Pareto solution, while f_i^{max} and f_i^{min} are the upper and lower limitations of the *ith* objective function, respectively.

A. PELICAN OPTIMIZATION ALGORITHM

The POA is an innovative stochastic optimization approach based on natural inspiration [22]. It is acknowledged for its superior ability to explore and exploit the search space in pursuit of the global optimum. Swarm-inspired algorithms have garnered significant attention recently and the POA is specifically influenced by the foraging strategy and behaviour of pelicans. In nature, pelicans often collaborate when hunting and their approach involves several steps. Upon distinguishing the location of their prey, they execute a synchronised dive followed by the expansion of their wings. This action compels their prey to rise to the water's surface and move into shallower areas, making it easier for the pelicans to capture their quarry. The fundamental stages of the POA are delineated as follows:

1) INITIALIZATION

The POA, functioning as a population-based algorithm, considers each member within the pelican group a potential solution. The optimization procedure commences with the random initialization of each member in the population, a process facilitated by the following equation:

$$X_{i,j} = LB_j + rand * \left(UB_j - LB_j\right) i = 1, 2, \ldots, N, \quad j = 1, 2, \ldots, M \tag{15}$$

where, $X_{i,j}$ is the jth variable's value according to the ith candidate solution, N is the quantity of members in the population, M is the quantity of problematic variables, rand is the random quantity of intervals [0 1], LB_j is the inferior boundary of the *jth*, and UB_j is the superior boundary of the *jth* of the problematic variables.

2) PHASE 1 (EXPLORATION): MOVING TOWARDS FOOD SOURCES

The initial stage mirrors the pelicans' approach to scanning the search space as they seek out their prey. Upon identification of the prey, the pelicans shift their focus towards its location. A noteworthy feature of the POA is its capacity to randomly generate the prey's location, thereby enhancing its exploration capabilities. The new position of the *ith* pelican candidate solution in Phase 1 is mathematically expressed as:

$$X_{i,j}^{P_1} = \begin{cases} X_{i,j} + rand.(P_j - I.X_{i,j}), & F_p < F_i; \\ X_{i,j} - rand.(P_j - I.X_{i,j} &), \text{else} \end{cases} \tag{16}$$

where, $X_{i,j}^{P_1}$ is the most recent position of the *ith* pelican in the *jth* dimension according to Phase 1, P_j is the position of the prey in the *jth* dimension, and F_p is the value of this objective function. The I parameter can randomly be either 1 or 2. For each iteration and every member, a parameter is randomly selected. When this parameter is set to a value of two, it induces greater displacement in a member's position, potentially leading that member to explore new regions within the search space. Thus, the I parameter significantly influences the exploration capability of the POA, enabling it to systematically scan the search space. Consequently, the solution is updated based on the new position, as outlined in the subsequent equation:

$$X_i = \begin{cases} X_i^{P_1}, & F_i^{P_1} < F_i; \\ X_i, & \text{eles,} \end{cases} \tag{17}$$

where, $X_i^{P_1}$ is the most recent position of the ith pelican and $F_i^{P_1}$ is the value of this objective function according to Phase 1.

3) PHASE 2 (EXPLOITATION): WINGING ON THE WATER SURFACE

In the second stage, upon reaching the surface of the water, the pelicans employ the strategy of extending their wings to corral fish upwards. Fish coerced to the water's surface are then gathered in the pelicans' throat pouch. This approach results in a higher number of fish captured within the targeted area. Incorporating this pelican behaviour into the proposed POA enhances its convergence towards more favourable points within the hunting area, thereby, boosting its local search capabilities and exploitation efficiency. From a mathematical perspective, the algorithm is required to scrutinise the points in the vicinity of the pelican's location to converge towards an improved solution. This emulation of pelican behaviour during hunting is mathematically expressed as:

$$X_{i,j}^{P_2} = X_{i,j} + R \cdot (1 - t/t_{Max}) \cdot (2 \cdot rand - 1) \cdot X_{i,j}, \quad (18)$$

where, $X_{i,j}^{P_2}$ is the most recent position of the ith pelican in the *jth* dimension according to Phase 2, R is a constant that is set at 0.2, t is the present iteration, and t_{Max} is the maximal quantity of iterations. The coefficient "$R \cdot (1 - t/t_{Max})$" serves as an indicator of the neighbourhood radius around each population member, allowing for local search efforts in proximity to each member, thus, boosting the arrival to an enhanced solution. Subsequently, the solution is updated based on the new position, as specified in the following equation:

$$X_i = \begin{cases} X_i^{P_2}, F_i^{P_2} < F_i; \\ X_i, \text{eles}, \end{cases} \quad (19)$$

where, $X_i^{P_2}$ is the latest position of the ith pelican and $F_i^{P_2}$ is the value of this objective function according to Phase 2.

B. IMPROVED PELICAN OPTIMIZATION ALGORITHM

Phase 2 of the original POA is refined in the IPOA. For the IPOA, we introduced a dynamic weighting technique, through which the weight parameter is adaptively adjusted with each iteration. This strategic adaptive adjustment bolsters the algorithm's convergence and elevates the overall quality of the solution. With this enhanced version, the weight 'w' is iteratively tweaked to establish a balance between exploration and exploitation within Phase 2 of the algorithm. The updated equation is expressed as follows:

$$X_{i,j}^{P_2} = X_{i,j} + W \cdot (1 - t/t_{Max}) \cdot (2 \cdot rand - 1) \cdot X_{i,j}, \quad (20)$$

In this framework, W serves as a parameter which governs the scales of the search throughout the iterative process. This process commences with a substantial value, roughly a quarter of the standard search domain scaling, which gradually diminishes to approximately 1% of the quarter of this length. We observed that the stability of the POA is boosted by the following monotonically decreasing function:

$$W = ((W_o - W_\infty)/(1 - t_{Max})) \times (t - t_{Max}) + W_\infty \quad (21)$$

Here, W_o and W_∞ signify the initial and final values, respectively. Essentially, W assumes control over the iteration procedure. Generally, W_o and W_∞ can be set as follows:

$$W_o = (UB - LB)/4 \quad (22)$$

$$W_\infty = W_o/100 \quad (23)$$

where, t is the present iteration, t_{Max} is the maximal quantity of iterations, while UB and LB are the superior and inferior boundaries, respectively.

At the commencement of the iterative process, W begins with a significant value, facilitating the random movements of pelicans. This stimulates increased exploration capabilities within the algorithm, enabling more effective exploration of the entire search space. Towards the conclusion of the iterative process, W's value decreases, thereby, reducing the search region around the best solution. This, in turn, heightens the exploitation capabilities of the algorithm. In comparison to the original POA, this improved version delivers an improved convergence speed together with an enhanced solution quality. The different stages of the IPOA are depicted in the flowchart provided in Figure 2.

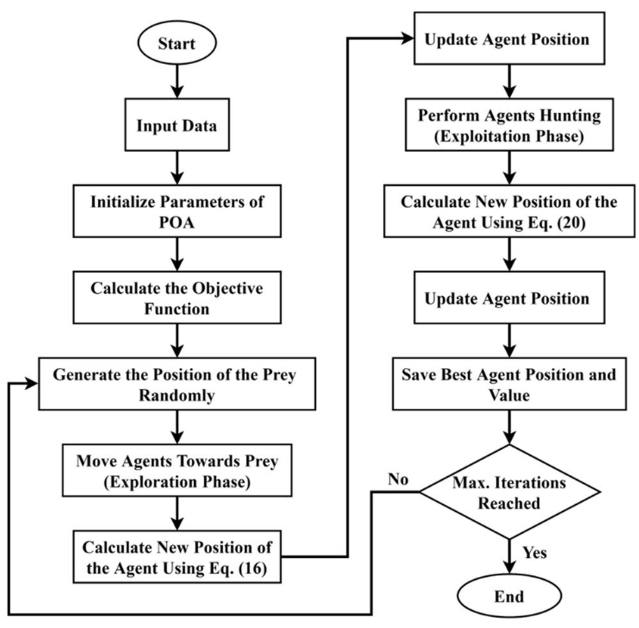

FIGURE 2. The IPOA stages flowchart.

IV. SIMULATION RESULTS

During this study, we assessed a grid-connected NG system that incorporates a PV array and three BSDs functioning collectively as a BSD unit, the proposed NG has been designed in MATLAB Simulink in previous work by the authors [3], then the output data is transferred to workspace to be as an input to the proposed algorithm in the current study. To gauge the effectiveness of the IPOA in resolving the challenge of optimal NG operation within a multi-objective framework, we subjected this algorithm to three distinct scenarios. In Scenario 1, we considered unrestricted power exchange with the primary grid, while in Scenario 2 we set a predefined limit on power exchange between the NG system and the main grid and in Scenario 3, we assumed that PV array operating at the maximum capacity. Additionally, we conducted a comparative analysis to weigh the performance of the IPOA against that of the POA, IDE, and the bat algorithm within all the situations mentioned above. The optimization algorithms were standardized with a population size and maximum iteration set at 50 and 100 respectively. In IPOA and POA, the parameter I set at 2. In the IDE algorithm, mutation and crossover were designated as 0.1 and 0.8, while for the Bat algorithm, loudness and pulse were chosen as 0.9 and 0.98 [23], based on experimental outcomes to enhance solution quality. This study adheres to the Levelized Cost of Energy (LCOE) standards set by the International Renewable Energy Agency (IRENA), measured in USD/kWh for PV systems. As the LCOE is contingent on geographic and country-specific factors, the data utilized for this study is consistent with the situation in Malaysia. The LCOE covers installation costs as well as the operational and maintenance (O&M) expenses associated with the power source. Additionally, the real cost of BSD usage, in terms of USD/kWh, was computed by spreading its cost (following IRENA standards, which is USD 135/kWh) across its usable life. The usable life was ascertained by multiplying the cycle life (3000 cycles) by the BSD's rated energy content (4.8 kWh). To prevent overcharging and over-discharging, the state of charge (SOC) for each battery is constrained to a range of 20% minimum SOC to 80% maximum SOC, while initial_SOC were set at 50%. Table 1 depicts the cost coefficients (USD/kWh), the CO_2 emission factor (kg/kWh) for Malaysian grids based on the International Energy Agency (IEA) [24], theBSD CO_2 emission factors [5], and the maximum and minimum production of every source. Table 2 depicts a random commercial load profile for a 24-hour period while Table 3 displays the 24-hour electricity purchase prices (USD/kWh) from the country's national grid [25]. These prices are in accordance with the conventional commercial rates set by Malaysia electric utility, Tenaga Nasional Berhad (TNB). It is assumed that the electricity selling price (in USD/kWh) to the main grid is set 20% lower than the purchasing price, as shown in Table 4. The PV power generation data is provided in Table 5, The analysis incorporates historical irradiation data of one day for Malaysia and assumes a PV temperature of 25°C.

A. UNLIMITED POWER EXCHANGE WITH THE MAIN GRID (SCENARIO 1)

In this particular situation, we assume that the PV system and BSDs operate within their designated power limits, whereas the main grid operates without any constraints, freely exchanging power with the NG system. The simulation outcomes for this scenario with the utilization of the IPOA are shown in Table 6. To highlight the efficacy of the IPOA,

TABLE 1. The cost, resource emission factor, and maximal as well as minimal energy production.

Source	Cost (USD/kWh)	CO_2 Emission Factor (kg/kWh)	P_{MIN} (kW)	P_{MAX} (kW)
PV	0.078	0	0	16.7
Battery	0.045	0.01	-4.8	4.8
Grid	According to the tables 3 and 4.	0.749	-10	10

TABLE 2. The load profile for a one-day period.

Time (h)	Power (kW)	Time (h)	Power (kW)
1	3.011	13	9.413
2	2.864	14	9.217
3	2.612	15	10
4	2.573	16	9.673
5	2.671	17	9.043
6	2.787	18	7.458
7	2.909	19	5.554
8	2.876	20	4.356
9	4.835	21	4.924
10	7.92	22	4.538
11	8.866	23	4.351
12	8.906	24	4.219

TABLE 3. The buying price of energy from the main grid for a period of one day.

Time (h)	Price (USD/kWh)	Time (h)	Price (USD/kWh)
1	0.067	13	0.085
2	0.067	14	0.14
3	0.067	15	0.14
4	0.067	16	0.14
5	0.067	17	0.085
6	0.067	18	0.085
7	0.067	19	0.085
8	0.085	20	0.085
9	0.085	21	0.085
10	0.085	22	0.067
11	0.14	23	0.067
12	0.085	24	0.067

TABLE 4. The selling price of energy to the main grid for a period of one day.

Time (h)	Price (USD/kWh)	Time (h)	Price (USD/kWh)
1	0.0536	13	0.068
2	0.0536	14	0.112
3	0.0536	15	0.112
4	0.0536	16	0.112
5	0.0536	17	0.068
6	0.0536	18	0.068
7	0.0536	19	0.068
8	0.068	20	0.068
9	0.068	21	0.068
10	0.068	22	0.0536
11	0.112	23	0.0536
12	0.068	24	0.0536

TABLE 5. The amount of energy generated by the PV array in one day.

Time (h)	Power (kW)	Time (h)	Power (kW)
1	0	13	15.928
2	0	14	14.28
3	0	15	11.314
4	0	16	7.4909
5	0	17	2.9568
6	0	18	0.017231
7	1.2225	19	0
8	5.1682	20	0
9	10.771	21	0
10	13.988	22	0
11	15.902	23	0
12	16.604	24	0

we applied it to address the problem, generating a Pareto Front comprising a variety of optimal solutions. The Pareto Front is then compared with the results obtained by way of the original POA, IDE, and the bat algorithms, as depicted in Figures 3,4,5, and 6. The objectives, which encompass operating costs and CO_2 emissions, are essentially conflicting. As portrayed in Figure 3,4,5, and 6, the movement from initial points on the graphs to the end points as well as along the Pareto path is an indication of alterations in the operational pattern. This transformation spans from situations characterised by lower costs and higher emissions to those with greater costs and lower emissions. An assessment of the IPOA against other algorithms, in terms of optimal cost and CO_2 emission as well as the proportion of energy generation from each source, is depicted in Table 7.

TABLE 6. The distribution of energy post-application of the IPOA (scenario 1).

Time (h)	PV (kW)	Bat 1 (kW)	Bat 2 (kW)	Bat 3 (kW)	Grid (kW)
1	0	2.11646	2.11646	2.11646	-3.24968
2	0	2.24856	2.24856	2.24856	-3.77121
3	0	2.08867	2.08867	2.08867	-3.56534
4	0	2.44840	2.44840	2.44840	-4.65915
5	0	2.62139	2.62139	2.62139	-5.08743
6	0	2.70573	2.70573	2.70573	-5.24082
7	1.17655	3.34194	3.34194	3.34194	-8.19057
8	2.91966	1.40142	1.40142	1.40142	-4.21632
9	10.0683	1.67699	1.67699	1.67699	-10.0541
10	5.78823	1.72663	1.72663	1.72663	-2.87447
11	15.902	-2.28467	-2.28467	-2.28467	-0.0383
12	3.17641	1.98024	1.98024	1.98024	0.105229
13	1.42383	1.59683	1.59683	1.59683	3.227647
14	14.1	2.54607	2.54607	2.54607	-12.1421
15	11.314	-2.15961	-2.15961	-2.15961	5.399961
16	7.4909	3.42012	3.42012	3.42012	-7.84087
17	2.14417	-3.01922	-3.01922	-3.01922	16.10613
18	0.00043	3.71432	3.71432	3.71432	-3.38127
19	0	-3.02036	-3.02036	-3.02036	14.88529
20	0	2.54158	2.54158	2.54158	-3.09842
21	0	-3.15813	-3.15813	-3.15813	14.50464
22	0	3.08259	3.08259	3.08259	-4.53331
23	0	-3.56998	-3.56998	-3.56998	15.1923
24	0	1.98233	1.98233	1.98233	-1.62949

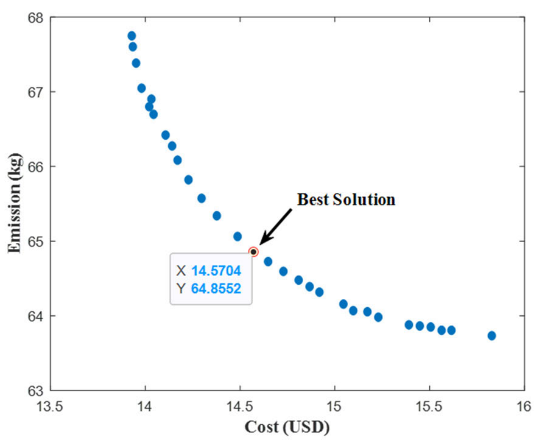

FIGURE 3. The distribution of the operating cost and CO_2 emission, according to IDE algorithm with the pareto criterion (scenario 1).

B. SPECIFIED LIMIT POWER EXCHANGE WITH THE MAIN GRID (SCENARIO 2)

In this segment, we address the multi-objective problem, covering operational costs and CO_2 emission. We take into

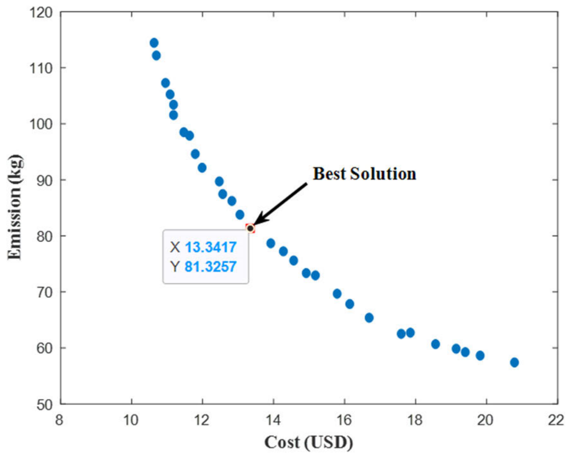

FIGURE 4. The distribution of the operating cost and CO_2 emission, according to bat algorithm with the pareto criterion (scenario 1).

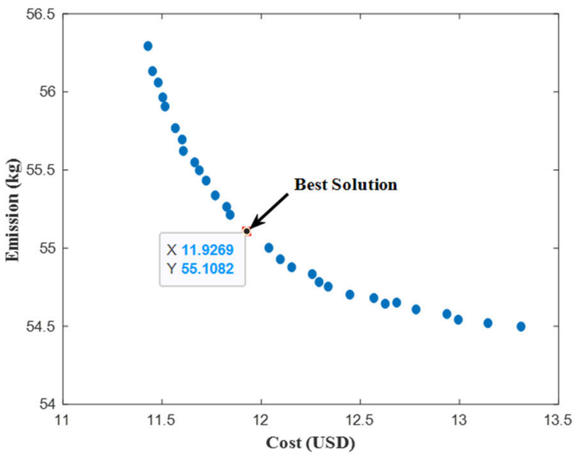

FIGURE 5. The distribution of the operating cost and CO_2 emission, according to POA algorithm with the pareto criterion (scenario 1).

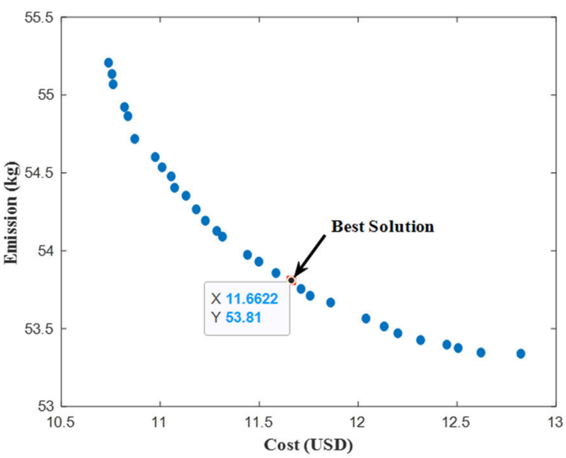

FIGURE 6. The distribution of the operating cost and CO_2 emission, according to IPOA algorithm with the pareto criterion (scenario 1).

account the prescribed power exchange limits between the NG; which comprises the BSDs and PV array; and the primary grid, as specified in Table 1. Table 8 depicts the optimal

TABLE 7. A comparison of the percentage of energy generated by each resource with the best solution (scenario 1).

Optimization Algorithm	Optimal Cost (USD)	Optimal CO_2 Emission (kg)	PV Array (%)	Battery Bank (%)	Grid (%)
IDE	14.5704	64.8552	26.94	44.2	28.84
Bat Algorithm	13.3417	81.3257	27.25	29.03	43.71
POA	11.9269	55.1082	29.81	44.1	26.08
IPOA	11.6622	53.81	27.49	47.22	25.27

24-hour generation schedule, aimed at reducing both cost and CO_2 emission by way of the IPOA. The proposed algorithm was employed to assess its Pareto Front in comparison to the original POA, IDE, and bat algorithms, as illustrated in Figures 7,8,9, and 10. The simulation findings revealed that during the initial hours of the day, the BSDs delivered the NG load in accordance with increased market prices. Contrastingly, the PV unit prioritised cost and emission constraints as it began supplying the load. Meanwhile, the procurement of energy from the main grid was more prevalent during late hours, when prices were favourable, serving load needs and battery recharging. The NG predominantly sold surplus energy to the main grid during the early and midday hours, capitalising on high selling prices to realise enhanced economic efficiency. For Scenario 2, a comparison between the IPOA and other algorithms, in terms of optimal cost and CO_2 emission, as well as the percentage of generation for each unit, can be observed in Table 9.

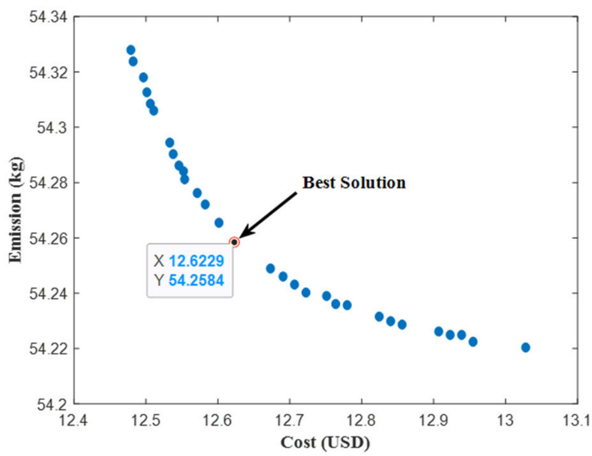

FIGURE 7. The distribution of the operating cost and CO_2 emission, according to IDE algorithm with the pareto criterion (scenario 2).

C. OPERATING AT THE MAXIMUM CAPACITY OF PV SOURCE (SCENARIO 3)

In this particular case, we operated under the assumption that the PV source functions at its maximum power capacity. The numerical results obtained from the simulation, employing

TABLE 8. The distribution of energy post-application of the IPOA (scenario 2).

Time (h)	PV (kW)	Bat 1 (kW)	Bat 2 (kW)	Bat 3 (kW)	Grid (kW)
1	0	2.87121	2.87121	2.87121	-5.4652
2	0	2.44196	2.44196	2.44196	-4.3619
3	0	1.92276	1.92276	1.92276	-3.06197
4	0	0.85864	0.85864	0.85864	0.003495
5	0	2.24057	2.24057	2.24057	-3.96929
6	0	2.56516	2.56516	2.56516	-4.88431
7	0.91439	2.66154	2.66154	2.66154	-5.90449
8	2.76498	1.15017	1.15017	1.15017	-3.22231
9	7.71850	-0.19415	-0.19415	-0.19415	-2.24303
10	11.7979	2.13252	2.13252	2.13252	-10
11	15.902	-0.31284	-0.31284	-0.31284	-5.69484
12	12.1393	2.30021	2.30021	2.30021	-10
13	13.4512	2.06395	2.06395	2.06395	-10
14	14.1	1.84286	1.84286	1.84286	-10
15	11.314	3.05322	3.05322	3.05322	-10
16	7.4909	-2.56962	-2.56962	-2.56962	9.98383
17	0.84977	2.73553	2.73553	2.73553	-0.01004
18	0.01524	-0.66057	-0.66057	-0.66057	9.650388
19	0	-1.31621	-1.31621	-1.31621	9.642262
20	0	-1.84319	-1.84319	-1.84319	9.973164
21	0	3.06611	3.06611	3.06611	-4.042
22	0	-1.77599	-1.77599	-1.77599	9.983746
23	0	-1.77962	-1.77962	-1.77962	9.779415
24	0	3.67859	3.67859	3.67859	-6.69014

TABLE 9. A comparison of the percentage of energy generated by each resource with the best solution (Scenario 2).

Optimization Algorithm	Optimal Cost (USD)	Optimal CO_2 Emission (kg)	PV Array (%)	Battery Bank (%)	Grid (%)
IDE	12.6229	54.2584	23.88	49.44	26.66
Bat Algorithm	12.6369	68.0104	27.06	33.34	39.59
POA	11.4171	54.7356	25.45	45.35	29.19
IPOA	10.5579	45.6443	36.43	41.72	21.83

the IPOA, are detailed in Table 10. To underscore the efficacy of the IPOA, it is utilized to tackle the problem, producing a diverse array of optimal solutions forming a Pareto Front. This Pareto Front is subsequently compared with outcomes from the original POA, IDE, and the Bat Algorithm,

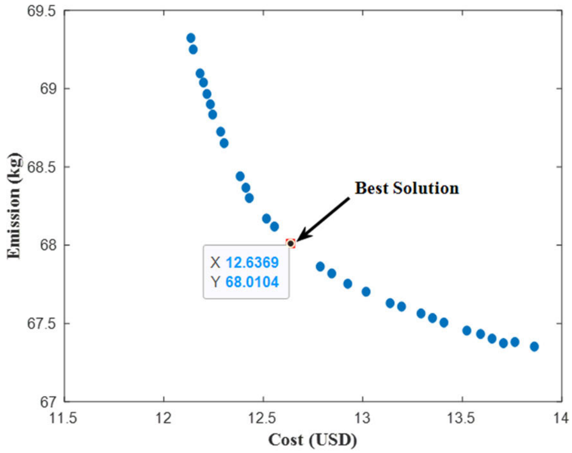

FIGURE 8. The distribution of the operating cost and CO_2 emission, according to Bat algorithm with the pareto criterion (scenario 2).

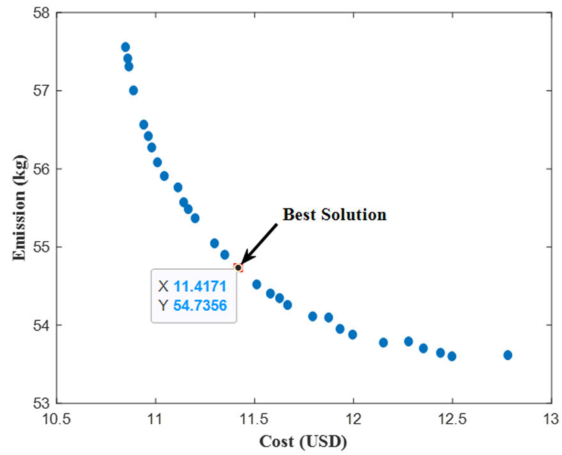

FIGURE 9. The distribution of the operating cost and CO_2 emission, according to POA algorithm with the pareto criterion (scenario 2).

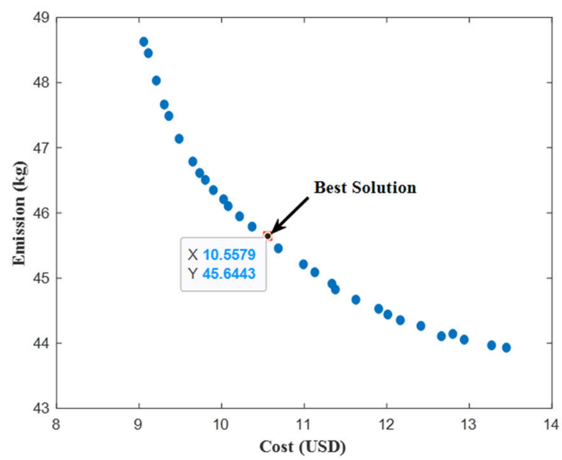

FIGURE 10. The distribution of the operating cost and CO_2 emission, according to IPOA algorithm with the pareto criterion (scenario 2).

as depicted in Figure 11,12,13, and 14. An assessment of the IPOA against other algorithms is shown in Table 11, focusing on optimal cost, CO_2 emissions, and the distribution of energy generation from each source.

TABLE 10. The distribution of energy post-application of the IPOA (scenario 3).

Time (h)	PV (kW)	Bat 1 (kW)	Bat 2 (kW)	Bat 3 (kW)	Grid (kW)
1	0	2.46750	2.46750	2.46750	-4.24276
2	0	2.84973	2.84973	2.84973	-5.56714
3	0	2.43130	2.43130	2.43130	-4.556
4	0	1.86824	1.86824	1.86824	-2.90607
5	0	2.38592	2.38592	2.38592	-4.39082
6	0	2.69912	2.69912	2.69912	-5.17433
7	1.2225	2.63376	2.63376	2.63376	-6.08838
8	5.1682	2.48658	2.48658	2.48658	-9.62306
9	10.771	2.81609	2.81609	2.81609	-14.2281
10	13.988	-1.53541	-1.53541	-1.53541	-1.26973
11	15.902	-0.46212	-0.46212	-0.46212	-5.25554
12	16.604	-1.76844	-1.76844	-1.76844	-2.00188
13	15.928	1.80478	1.80478	1.80478	-11.5198
14	14.1	2.46256	2.46256	2.46256	-12.0018
15	11.314	2.07094	2.07094	2.07094	-7.03873
16	7.4909	-2.90927	-2.90927	-2.90927	11.31131
17	2.9568	2.38259	2.38259	2.38259	-0.69501
18	0.01723	0.49302	0.49302	0.49302	6.025282
19	0	2.52611	2.52611	2.52611	-1.76437
20	0	-3.08276	-3.08276	-3.08276	13.61065
21	0	2.38250	2.38250	2.38250	-2.07423
22	0	-2.45833	-2.45833	-2.45833	12.02176
23	0	3.54165	3.54165	3.54165	-6.1182
24	0	-1.94457	-1.94457	-1.94457	10.18136

TABLE 11. A comparison of the percentage of energy generated by each resource with the best solution (scenario 3).

Optimization Algorithm	Optimal Cost (USD)	Optimal CO_2 Emission (kg)	PV Array (%)	Battery Bank (%)	Grid (%)
IDE	12.668	53.7667	35.44	43.35	21.19
Bat Algorithm	14.6939	74.3768	43.62	19.49	36.88
POA	13.2286	57.7726	35.31	41.91	22.77
IPOA	11.4373	41.4435	39.88	41.75	18.35

The pricing structure for electrical power purchases from the Malaysian grid comprises three distinct periods: off-peak, mid-peak, and peak. It is notable that during the mid-peak and peak hours, the prices are higher in comparison to the

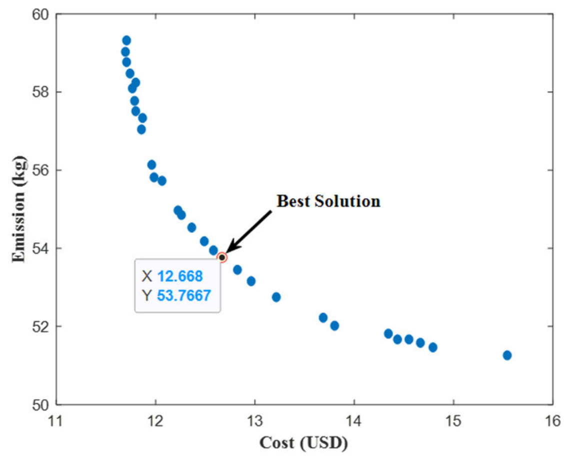

FIGURE 11. The distribution of the operating cost and CO_2 emission, according to IDE algorithm with the pareto criterion (scenario 3).

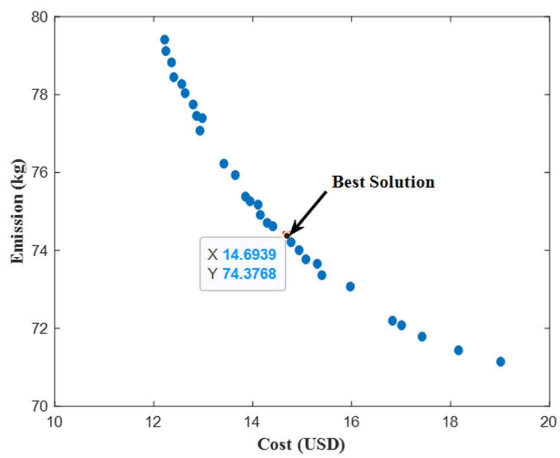

FIGURE 12. The distribution of the operating cost and CO_2 emission, according to Bat algorithm with the pareto criterion (scenario 3).

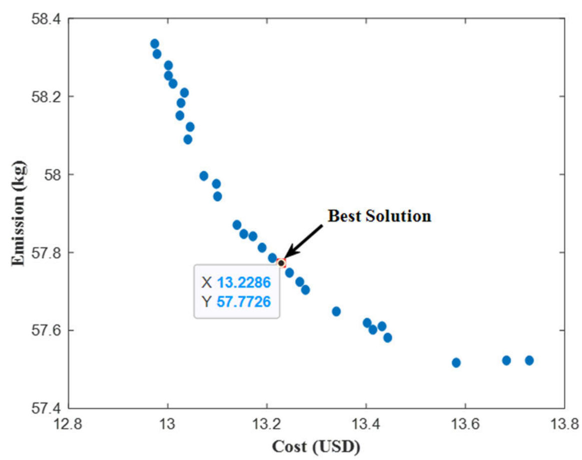

FIGURE 13. The distribution of the operating cost and CO_2 emission, according to POA algorithm with the pareto criterion (scenario 3).

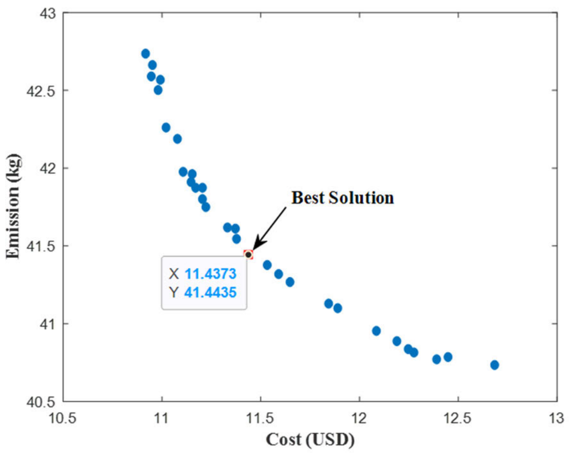

FIGURE 14. The distribution of the operating cost and CO_2 emission, according to IPOA algorithm with the Pareto criterion (Scenario 3).

rates of the PV array and BSDs. Conversely, during off-peak hours, the prices for power from the utility grid are lower. Also, the level of CO_2 emission from the grid is consistently above that of the BSDs at all times. Optimum power exchange between NG and the primary grid as well as optimum energy set points for PV and BSDs are crucial for minimizing both the CO_2 emission and operational costs for NG. In Scenario 1, NG procures a total of 69.41 kW from the main grid while selling 83.56 kW to the utility grid. Notably, in Scenario 2, the total power purchased from the main grid is 59.01 kW, with NG selling 99.54 kW to the utility grid. Finally, in Scenario 3, NG procures a total of 53.14 kW from the main grid with NG selling 106.41 kW to the utility grid. As such, in terms of minimizing both cost and CO_2 emission, Scenarios 2 and 3 are deemed more effective. Also, the simulation results revealed that, in Scenario 2, the implementation of a stipulated limit for power exchange between the main grid and NG while considering the environmental and economic objectives simultaneously led to a 15% reduction in NG CO_2 emission as well as a 9.5% reduction in operational costs. While, in Scenario 3, the operating at the maximum capacity of PV array with considering the environmental and economic objectives simultaneously led to a 23% reduction in NG CO_2 emission as well as a 2% reduction in operational costs in comparison with Scenario 1.

Figures (3-14), clearly show that, in terms determining the optimal balance between operating expenditure and CO_2 emission, the proposed IPOA outperforms the original POA, IDE, and bat algorithms in all scenarios. It achieved the best cost and CO_2 emission values of 11.6622 USD and 53.81 kg, respectively, in Scenario 1. In Scenario 2, the proposed IPOA delivered an operating cost of 10.5579 USD and a CO_2 emission of 45.6443 kg. while, in Scenario 3, the proposed algorithm achieved an operating cost of 11.4373 USD and a CO_2 emission of 41.4435 kg.

Given the stochastic nature of the proposed IPOA, like other stochastic optimization methods, it's crucial to acknowledge a limitation: there's no assurance that IPOA will consistently yield solutions precisely equal to the global optimum across all optimization problems. Consequently, the authors propose future research avenues, suggesting the application of IPOA across diverse scientific domains and real-world challenges. This encompasses employing the algorithm in areas like wireless sensor networks, image processing, signal denoising, power systems, machine learning, artificial intelligence, and various benchmark functions.

V. CONCLUSION

The focus of this study is on the enhancement and utilization, of the stochastic nature of the POA to optimize the management of NG. In this regard, two conflicting objectives need to be taken into consideration: the lowering of operational costs, and the reduction of CO_2 emission. The evaluation of total operational cost and CO_2 emission was executed in three different scenarios: unlimited power exchange (Scenario 1), constrained power exchange (Scenario 2) between the main grid and NG and operating at the maximum capacity of PV source (Scenario 3). As per the simulation findings, Scenario 2, featuring a defined limit on power exchange, and Scenario 3, involving the operation at the maximum capacity of the PV source, exhibit superiority in reducing operational costs (9.5% for Scenario 2 and 2% for Scenario 3), along with a reduction in CO_2 emissions (15% for Scenario 2 and 23% for Scenario 3). The effectiveness of the proposed IPOA was showcased by comparing its performance with that of the original POA, IDE and Bat algorithms.

REFERENCES

[1] M. F. Roslan, M. A. Hannan, P. J. Ker, R. A. Begum, T. I. Mahlia, and Z. Y. Dong, "Scheduling controller for microgrids energy management system using optimization algorithm in achieving cost saving and emission reduction," *Appl. Energy*, vol. 292, Jun. 2021, Art. no. 116883, doi: 10.1016/j.apenergy.2021.116883.

[2] X. Ma, Y. Mu, Y. Zhang, C. Zang, S. Li, X. Jiang, and M. Cui, "Multi-objective microgrid optimal dispatching based on improved bird swarm algorithm," *Global Energy Interconnection*, vol. 5, no. 2, pp. 154–167, Apr. 2022, doi: 10.1016/j.gloei.2022.04.013.

[3] S. Jamal, J. Pasupuleti, N. A. Rahmat, and N. M. L. Tan, "Energy management system for grid-connected Nanogrid during COVID-19," *Energies*, vol. 15, no. 7689, 2022, doi: 10.3390/en15207689.

[4] S. Jamal, N. M. L. Tan, and J. Pasupuleti, "A review of energy management and power management systems for microgrid and nanogrid applications," *Sustainability*, vol. 13, no. 18, p. 10331, Sep. 2021, doi: 10.3390/su131810331.

[5] M. Sedighizadeh, M. Esmaili, A. Jamshidi, and M.-H. Ghaderi, "Stochastic multi-objective economic-environmental energy and reserve scheduling of microgrids considering battery energy storage system," *Int. J. Electr. Power Energy Syst.*, vol. 106, pp. 1–16, Mar. 2019, doi: 10.1016/j.ijepes.2018.09.037.

[6] F. Qayyum, F. Jamil, S. Ahmad, and D.-H. Kim, "Hybrid renewable energy resources management for optimal energy operation in nano-grid," *Comput., Mater. Continua*, vol. 71, no. 2, pp. 2091–2105, 2022, doi: 10.32604/cmc.2022.019898.

[7] S. Basu and M. Basu, "Horse herd optimization algorithm for fuel constrained day-ahead scheduling of isolated nanogrid," *Appl. Artif. Intell.*, vol. 35, no. 15, pp. 1250–1270, Dec. 2021, doi: 10.1080/08839514.2021.1975392.

[8] P. Shamsi, H. Xie, A. Longe, and J.-Y. Joo, "Economic dispatch for an agent-based community microgrid," *IEEE Trans. Smart Grid*, vol. 7, no. 5, pp. 2317–2324, Sep. 2016, doi: 10.1109/TSG.2015.2487422.

[9] B. Dey, B. Bhattacharyya, and F. P. G. Márquez, "A hybrid optimization-based approach to solve environment constrained economic dispatch problem on microgrid system," *J. Cleaner Prod.*, vol. 307, Jul. 2021, Art. no. 127196, doi: 10.1016/j.jclepro.2021.127196.

[10] A. A. Moghaddam, A. Seifi, and T. Niknam, "Multi-operation management of a typical micro-grids using particle swarm optimization: A comparative study," *Renew. Sustain. Energy Rev.*, vol. 16, no. 2, pp. 1268–1281, Feb. 2012, doi: 10.1016/j.rser.2011.10.002.

[11] G. Aghajani and N. Ghadimi, "Multi-objective energy management in a micro-grid," *Energy Rep.*, vol. 4, pp. 218–225, Nov. 2018, doi: 10.1016/j.egyr.2017.10.002.

[12] H. Razmi and H. Doagou-Mojarrad, "Comparative assessment of two different modes multi-objective optimal power management of micro-grid: Grid-connected and stand-alone," *IET Renew. Power Gener.*, vol. 13, no. 6, pp. 802–815, Apr. 2019, doi: 10.1049/iet-rpg.2018.5407.

[13] M. Jaszczur, Q. Hassan, P. Palej, and J. Abdulateef, "Multi-objective optimisation of a micro-grid hybrid power system for household application," *Energy*, vol. 202, Jul. 2020, Art. no. 117738, doi: 10.1016/j.energy.2020.117738.

[14] A. Fathy, T. M. Alanazi, H. Rezk, and D. Yousri, "Optimal energy management of micro-grid using sparrow search algorithm," *Energy Rep.*, vol. 8, pp. 758–773, Nov. 2022, doi: 10.1016/j.egyr.2021.12.022.

[15] M. A. Majeed, S. Phichaisawat, F. Asghar, and U. Hussan, "Optimal energy management system for grid-tied microgrid: An improved adaptive genetic algorithm," *IEEE Access*, vol. 11, pp. 117351–117361, 2023, doi: 10.1109/ACCESS.2023.3326505.

[16] M. Purlu and B. E. Turkay, "Optimal allocation of renewable distributed generations using heuristic methods to minimize annual energy losses and voltage deviation index," *IEEE Access*, vol. 10, pp. 21455–21474, 2022, doi: 10.1109/ACCESS.2022.3153042.

[17] M. Ghiasi, T. Niknam, M. Dehghani, P. Siano, H. H. Alhelou, and A. Al-Hinai, "Optimal multi-operation energy management in smart microgrids in the presence of RESs based on multi-objective improved DE algorithm: Cost-emission based optimization," *Appl. Sci.*, vol. 11, no. 8, p. 3661, Apr. 2021, doi: 10.3390/app11083661.

[18] S. Sun, C. Wang, Y. Wang, X. Zhu, and H. Lu, "Multi-objective optimization dispatching of a micro-grid considering uncertainty in wind power forecasting," *Energy Rep.*, vol. 8, pp. 2859–2874, Nov. 2022, doi: 10.1016/j.egyr.2022.01.175.

[19] M. R. B. Khan, R. Jidin, and J. Pasupuleti, "Multi-agent based distributed control architecture for microgrid energy management and optimization," *Energy Convers. Manage.*, vol. 112, pp. 288–307, Mar. 2016, doi: 10.1016/j.enconman.2016.01.011.

[20] A. M. Ameen, J. Pasupuleti, and T. Khatib, "Simplified performance models of photovoltaic/diesel generator/battery system considering typical control strategies," *Energy Convers. Manage.*, vol. 99, pp. 313–325, Jul. 2015, doi: 10.1016/j.enconman.2015.04.024.

[21] C. Lin and M. Gen, "Multi-criteria human resource allocation for solving multistage combinatorial optimization problems using multiobjective hybrid genetic algorithm," *Expert Syst. Appl.*, vol. 34, no. 4, pp. 2480–2490, May 2008, doi: 10.1016/j.eswa.2007.04.016.

[22] P. Trojovský and M. Dehghani, "Pelican optimization algorithm: A novel nature-inspired algorithm for engineering applications," *Sensors*, vol. 22, no. 3, p. 855, Jan. 2022.

[23] X. S. Yang, "A new metaheuristic bat-inspired algorithm," in *Nature Inspired Cooperative Strategies for Optimization* (Studies in Computational Intelligence). Berlin, Germany: Springer, 2010, pp. 65–74., doi: 10.1007/978-3-642-12538-6_6.

[24] M. A. Hannan, M. G. M. Abdolrasol, M. Faisal, P. J. Ker, R. A. Begum, and A. Hussain, "Binary particle swarm optimization for scheduling MG integrated virtual power plant toward energy saving," *IEEE Access*, vol. 7, pp. 107937–107951, 2019, doi: 10.1109/ACCESS.2019.2933010.

[25] N. A. M. Azman, M. P. Abdullah, M. Y. Hassan, D. M. Said, and F. Hussin, "Enhanced time of use electricity pricing for commercial customers in Malaysia," *Pertanika J. Sci. Technol.*, vol. 25, pp. 285–294, Jan. 2017.

SAIF JAMAL was born in Baghdad, Iraq. He received the Bachelor of Engineering degree from the Al Mamoun University College, Baghdad, in 2014, and the Master of Engineering degree from Universiti Kebangsaan Malaysia, in 2019. He is currently pursuing the Ph.D. degree in electrical power engineering with Universiti Tenaga Nasional, Kajang, Malaysia. His research interests include renewable energy sources, energy management systems, and power conversion systems.

JAGADEESH PASUPULETI (Senior Member, IEEE) is currently the Head of Hybrid Renewable Energy System with the Institute of Sustainable Energy, Universiti Tenaga Nasional, Malaysia. He is a member of IET, U.K., EI, U.K., BEM, Malaysia, MBOT, Malaysia, and ISTE, India; a Chartered Engineer, U.K.; a Professional Review Interviewer for C.Eng., U.K.; and a Professional Technologist, Malaysia. He has 36 years of teaching, research, and administrative experience. He has taught many subjects in electrical and electronics engineering both at undergraduate and postgraduate level. He has also supervised 35 postgraduate students. He has presented and published 150 papers in international conferences and international journals. He was an international program committee member, the session chair, and a reviewer of international conferences and Elsevier journals on power and energy systems area. He was also a keynote speaker in national and international conferences. He was involved in 60 research and consultancy projects funded around $ 5 million in renewable energy and energy efficiency.

NUR AZZAMMUDIN RAHMAT received the Ph.D. degree in electrical engineering from Universiti Teknologi MARA, Malaysia, in 2016, in the field of power system optimal dispatch. He is currently a Senior Lecturer with the College of Engineering, Universiti Tenaga Nasional, Malaysia. His current research interests include smart grids, smart city, renewable energy, power system analysis, and computational intelligence.

NADIA M. L. TAN (Senior Member, IEEE) was born in Kuala Lumpur, Malaysia. She received the B.Eng. degree (Hons.) in electrical engineering from the University of Sheffield, Sheffield, U.K., in 2002, the M.Eng. degree in electrical engineering from Universiti Tenaga Nasional, Kajang, Malaysia, in 2007, and the Ph.D. degree in electrical engineering from Tokyo Institute of Technology, Tokyo, Japan, in 2010.

She was an Associate Professor with the Department of Electrical and Electronics Engineering, Universiti Tenaga Nasional, from 2017 to 2021. From October 2016 to March 2017, she was a Visiting Researcher with the Power Electronics Laboratory, Tokyo Institute of Technology, where she was an Adjunct Associate Professor, from July 2016 to September 2016. She is currently an Associate Professor with the Department of Electrical and Electronics Engineering, University of Nottingham, Ningbo, China. Her research interests include power conversion systems for renewable energy and battery energy storage applications and bidirectional isolated DC–DC converters.

Dr. Tan is a registered Chartered Engineer with the Engineering Council, U.K., a registered Professional Engineer with the Board of Engineers Malaysia, and a member of the Institution of Engineering and Technology and the Institution of Engineers Malaysia. She is also a fellow of the Higher Education Academy. She was a recipient of the 2018 IET Young Engineer Award and 2018 IPCC IEEE IAS Prize Paper Award. She served as the Vice-Chair for the IEEE Power Electronics Society Malaysia Chapter, from 2018 to 2019.